JOURNAL OF SPACECRAFT AND ROCKETS
Vol. 34, No. 1, January–February 1997

Low-Earth-Orbit Micrometeoroid and Debris Investigations

L. Berthoud*
European Space Agency, 2200 AG Noordwijk, The Netherlands
and
J. C. Mandeville†
ONERA, 31400 Toulouse, France

The aim of this work is to improve current knowledge of micrometeoroids and orbital debris in low Earth orbit using space detection experiments. In 1990 and 1993, a series of samples exposed to the space environment for several years aboard the NASA Long Duration Exposure Facility and the Mir Orbital Station were retrieved. The samples were scanned to examine crater/perforation morphology and size distributions. The predicted flux on both experiments also was modeled using Kessler's debris and Grün's meteoroid distributions. To interpret the flux observed by the experiments, impact equations were needed to convert observed crater dimensions to impacting particle dimensions. Simulation experiments carried out in the laboratory showed that the Cour-Palais empirical equation was suitable. Further experiments demonstrated the influence of impact angle upon crater morphology. The results of the simulations together with the flux distribution on the Mir experiment indicated that secondary impacting might have occurred. Even without secondary impacts, the flux on Mir was significantly higher than model predictions.

Nomenclature

a = ellipse major axis length, cm
b = ellipse minor axis length, cm
Ci = ellipse circularity, b/a
c_t = velocity of sound in target, km/s
D = crater diameter, cm
d = particle diameter, cm
f = foil/target thickness, cm
H = Brinell hardness
P = penetration depth, cm
V = velocity of impact, km/s
α = impact angle, deg from normal
ε = foil ductility
ρ_p = density of projectile, g/cm^3
ρ_t = density of target or foil, g/cm^3
σ_{Al} = tensile strength of aluminum, 80 MPa for 6061-T6 Al
σ_t = tensile strength of target, MPa

Introduction

BEFORE the space age, knowledge of the space particulate environment was based upon the Earth-bound study of the zodiacal light, meteors, comets, asteroids, and meteorites. Since then, several methods have been developed to collect particle data from space itself.[1] The simplest of these methods is to expose a surface to the space environment, return it to Earth, and examine it for impacts. Micrometeoroid impacts at very high velocities produce characteristic craters in the samples. These craters can be analyzed to obtain information about the particles that caused them. The first microcraters found on experiments specifically designed for satellites were recovered from the Gemini[2] and Skylab missions.[3] Other recovered surfaces with microcraters were Apollo windows,[4] the Surveyor III camera,[5] and lunar rocks.[6] These samples helped to establish the natural particle flux, or number of particles impacting a certain area over a given time.

Whipple first used meteor and Pegasus and Explorer data to describe the flux of interplanetary objects.[7] Cour-Palais produced the next meteoroid environment model, which was frequently used.[8] Zook pointed out that satellite sensors could be mistaking artificial debris impacts for meteoroids and that lunar data were dominated by secondary ejecta craters for pit diameters below 7 μm (Ref. 9). Then, taking these factors into account, Grün et al. developed a meteoroid flux model based on theoretical considerations, satellite-obtained meteoroid data (HEOS 2 and Pioneer 8 and 9), and lunar flux measurements.[10] The first experimental proof of artificial debris impacting spacecraft came from the S-149 experiment on Skylab. In 1976, analyses of Skylab craters showed evidence of aluminum impact particles.[11] After this, the main data used in developing models of the debris environment came from the analysis of impacted surfaces recovered from the Solar Maximum satellite in 1984 (Refs. 12 and 13). The model most often used is that developed by Kessler in 1985, which has been through several revisions.[14,15] Empirical impact equations are still needed to relate observed crater dimensions to particle dimensions that are used by the flux models.

To update and refine models and our description of the micrometeoroid and debris environment in low Earth orbit (LEO), experiments were mounted on the NASA satellite Long Duration Exposure Facility (LDEF) and outside the Russian space station Mir. The experiments were intended to monitor and collect particles in LEO. Unfortunately, the high impact velocity during collection often results in vaporization of the impact particle. To combat this phenomenon, the multilayer collection technique was proposed to decelerate impactors. The aim is for the particle to break through one or more foils and remain fragmented on the layer below.[16]

This work describes the scanning of LDEF and Mir samples for impactor feature flux, diameters, circularities and depths; some simulation experiments performed in the laboratory to quantify impact behavior; modeling of the particle flux on the surfaces; a discussion of the results; and some conclusions. In achieving these goals it was necessary to establish the effect of angle of incidence on crater shape, to assess multilayer particle detector design, and to select an empirical equation for the comparison of calculated and observed fluxes.

Flight Experiments

The samples come from two sources: an experiment mounted outside Mir and two experiments on LDEF. The Mir orbital station has been in orbit at an altitude of 350–450 km with an inclination of 51.6 deg since February 1986. The French module Echantillons was placed outside the station during the Franco-Russian mission Aragatz. It was deployed on Dec. 9, 1988, and recovered 13 months later.[17] Its average altitude during this time was 387 km. The module consisted of various experiments intended to investigate the space

Received Oct. 11, 1995; revision received Aug. 2, 1996; accepted for publication Aug. 7, 1996.

*Research Fellow, Materials and Processes Division; currently Mechanical Systems Engineer, Matra Marconi Space UK Ltd., P.O. Box 16, Filton, Bristol BS12 7YB, England, United Kingdom.

†Senior Research Engineer, Department of Space Technology, Centre d'Etudes et de Recherches de Toulouse.

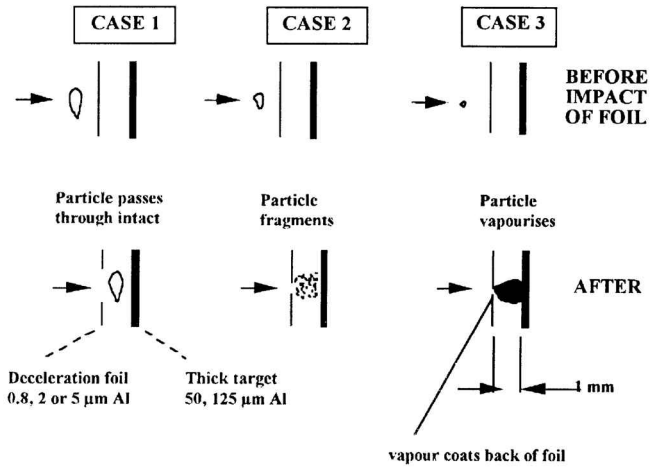

Fig. 1 Multiple foil collector principle.

environment. One of the experiments was a passive particle detector. The aim of this experiment was to investigate the feasibility of using multilayer thin-film detectors to collect micrometeoroids. One or more thin aluminum foils (of thicknesses ranging from 0.8 to 5 μm) were positioned in front of the main targets to act as selective detectors. Figure 1 shows what happens to the multilayer detector before and after impact when three different sizes of particles strike the foils.

The NASA LDEF was launched into LEO at 482-km altitude from the payload bay of the Space Shuttle Challenger in April 1984. It was retrieved from a 324-km-altitude orbit by the Shuttle Columbia after 69 months.[18] The satellite was a 14-sided, roughly cylindrical-shaped polygon, with a 5-m diam and 10-m-long aluminum frame. The experiments were stored in trays fixed to the aluminum frame. These trays faced in 14 directions, 12 along the sides (called rows) and 2 on the ends. During its mission, LDEF was stabilized with the long axis continually pointed toward the center of the Earth so that the rows remained at fixed angles relative to the direction of orbital motion. The French Cooperative Payload (FRECOPA) was positioned on the trailing edge, which was row 03. Two of the experiments were passive detectors dedicated to the study of dust particles. The microabrasion package (MAP) designed by the University of Kent was intended to measure the flux of the micrometeoroid environment and was situated on several different rows.[19] In this work the MAP aluminum foils on the leading surface (row 09) of LDEF were examined.

Scanning for Craters and Holes

When a high-velocity particle impacts a ductile surface, it produces either a crater or a hole, depending on the thickness of the sample. As these impact features are in general smaller than 1 mm, the samples are scanned with a microscope to find the craters. Optical microscopes, including a charge-coupled device video microscope, were used for an initial scan of the specimens. A Jeol JSM-840A scanning electron microscope (SEM) with energy dispersive x-ray (EDX) spectrometry capability was then used for detailed investigation of the features. Diameters were measured as the internal diameter at the sample surface. Depth was measured using stereoscopic photographs,[20] and circularity was calculated from the major and minor diameters (Fig. 2):

$$Ci = \pi b^2/\pi ab = b/a \qquad (1)$$

The circularity of a circle is unity, and as the obliquity increases, the circularity decreases.

Small errors in diameter measurement are inevitable, and some craters may be missed by the scanning process. The probability of the latter occurring increases as the limit of resolution is reached. For this work, craters down to about 1 μm in diameter could be seen consistently. Cumulative flux or crater size distributions are likely to be influenced by these errors by up to $\pm 20\%$ at the smallest sizes and much less at the larger sizes. Errors due to crater dimension measurement will probably be negligible compared with inaccurate

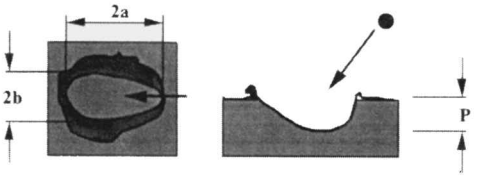

Fig. 2 Measurement of circularity and depth for oblique impacts.

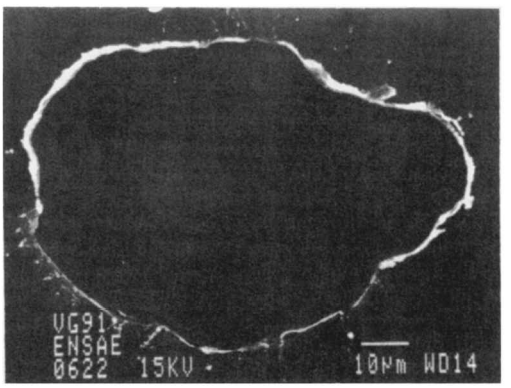

Fig. 3 Perforation of 5-μm-thick Mir foil shows particle shape.

fluxes produced by scanning too small an area. No error bars were put on the figures, which were considered busy enough.

Morphology of Observed Impact Features

A wide variation in morphology was seen for perforations on targets of different thickness. For thicker targets, the perforation lip appeared identical to a crater lip. As the target gets thinner, the lip thickness decreases until it is merely a bright outline around the hole. For very thin targets, where the ratio of crater diameter to foil thickness is greater than 20:1, the lip is virtually nonexistent, and the perforation diameter begins to approximate the particle diameter. This type of effect has also been noted by other investigators.[21] For these perforations, the perforations were no longer circular or symmetrical, but instead rather irregular (Fig. 3). The foil apparently acts as a witness to the shape of the particle as well as to its size. This would appear to confirm the finding from investigations of interplanetary dust particles that many of these particles are quite irregular in shape.[22] Figure 4 shows an example of the multiple foil detector operating correctly: the top image shows the hole through the top foil, and then on the second image the impact of the debris cloud on the front of the next foil down is seen. The last image shows an EDX spectrometry analysis to determine the elements present on the second foil. Analysis of the crystal in the middle shows the presence of Si, Mg, and Ca, which indicates the possibility of it being a meteoroid.

Elongated impacts that had one axis more than 10% longer than the other were considered to be caused by oblique impacts (i.e., coming from a direction not normal to the surface). Out of 162 impacts examined on the trailing edge of LDEF, 10% appeared to be caused by oblique impacts. On the Mir module, in general, 10–20% of the craters/perforations apparently came from obliques. These impacts were oblique in random directions. But on the part of the Mir module where a particularly high flux was observed (2.5×10^{-2} impacts/m^2/s for crater diameters larger than 1 μm), 35–50% of the craters were oblique and a large proportion of the oblique craters were uniform in direction. The circularity for these uniformly oriented oblique craters was an average of 0.79 with standard deviation of 0.06. This uniformity of direction implies that there may have been a single source of the impacts some distance away. This possibility is treated later in the Discussion.

Observed Flux Results

Table 1 gives a summary of the areas scanned with the SEM and the number of craters on semi-infinite surfaces and holes in thin films found on the different experiments. These figures cover several different data sets (further details are given in Ref. 23). The flux is

Table 1 Sample scanning details

	Area scanned, cm^2	Smallest crater seen, μm	No. of craters found
Mir			
0.8–50 μm Al	31	0.5	1583
LDEF FRECOPA			
250 μm Al	4	1.5	15
250 μm Al	20	3	17
250 μm Al	460	50	12
1 mm Al	3900	50	59
LDEF MAP			
25 μm thick Al	2.2	1	64
25 μm thick Al	26	5	107

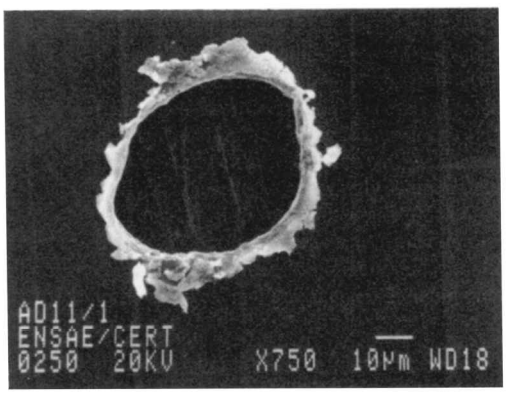

Fig. 4a LDEF D11/2 multiple foil detector, perforation of top foil (5-μm-thick Al).

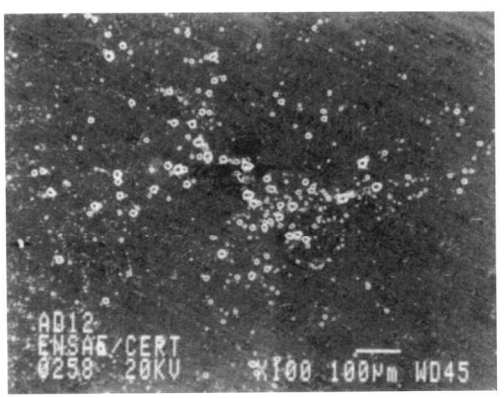

Fig. 4b Craters and fragments on the layer underneath the top foil (125-μm Al foil).

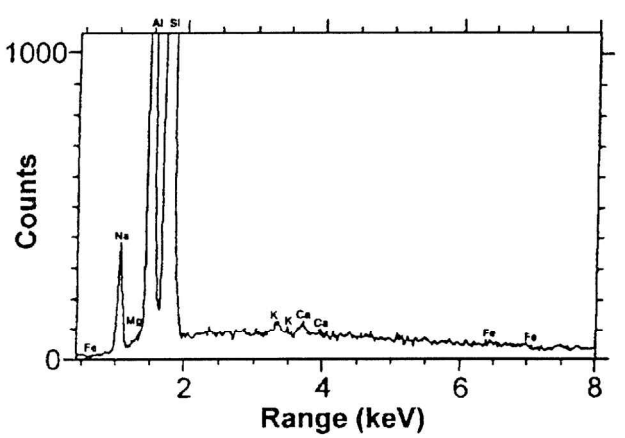

Fig. 4c Energy dispersive x-ray spectrum indicates presence of Al, Si, Na, Ca, and Mg.

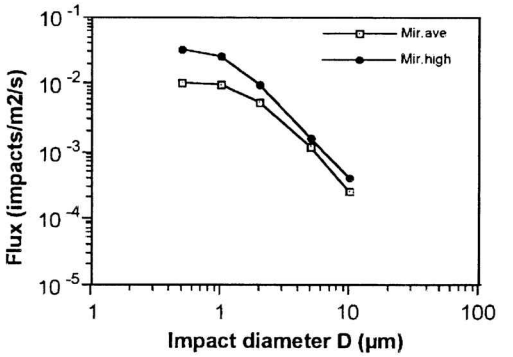

Fig. 5 Observed fluxes for Aragatz experiment on Mir.

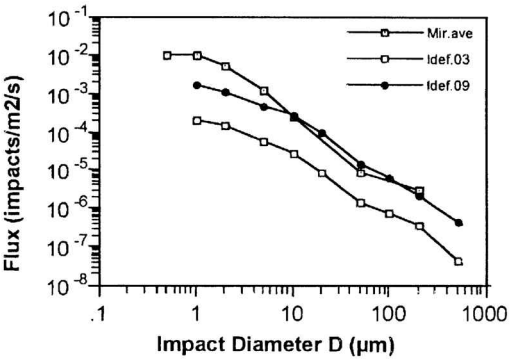

Fig. 6 Comparison between LDEF leading (09) and trailing (03) surfaces and the average observed Mir orbital station flux.

calculated by dividing the number of craters/area by the length of time the samples were exposed to the space environment: LDEF, 2105 days; and Mir, 385 days.

For the Mir experiment, a much higher flux was found on a certain area of one side of the experiment. The average of the flux found on these areas is compared with the average flux on the other samples in Fig. 5. Mir.ave represents the average flux, and Mir.high represents the higher flux seen on some samples. To simplify comparisons, all fluxes were taken from thick samples (i.e., 5 or 50 µm thick aluminum foils). Elemental analysis using EDX techniques revealed no evidence of remnants of impactors in these impact features.

For LDEF, flux results for the leading and trailing surfaces (rows 09 and 03) are shown in Fig. 6, and they are compared with the average flux observed on Mir. All flux measurements were made on thick aluminum targets. The leading-surface flux is approximately 10 times greater than that seen on the trailing surface. The average Mir flux is definitely higher than the LDEF leading edge for craters of diameter less than 10 μm.

Ground Simulation Experiments

Two sets of ground simulation experiments were carried out to choose a suitable empirical equation and to investigate the influence of impact angle on crater morphology. The first set of experiments was used to select a suitable empirical equation to permit a comparison between modeled and observed fluxes (see the Appendix to compare forms of existing empirical equations). Testing was done at both ends of the possible particle size range. The micron end of the range was tested by accelerating iron projectiles of 0.4–4 μm at velocities from 1–14 km/s into 50-μm aluminum (99% pure) foils, using the 2-MV electrostatic accelerator at the Max Planck Institut (MPI) für Kernphysik in Heidelberg. The millimeter end of the range was tested by accelerating 5-mm-diam steel spheres from 4 to 8 km/s into 10-cm-thick aluminum (6061-T6) block, with the two-stage light gas gun at the Centre d'Etudes de Gramat. Iron and steel projectiles were chosen as they are the easiest to accelerate and observe.

The targets were removed from the guns and scanned, and the impact features were measured. Figure 7 shows a comparison of experimental values of D/d with calculated values derived using different empirical equations given with references in the Appendix. As the equations are expressed in terms of P/d, it is necessary to

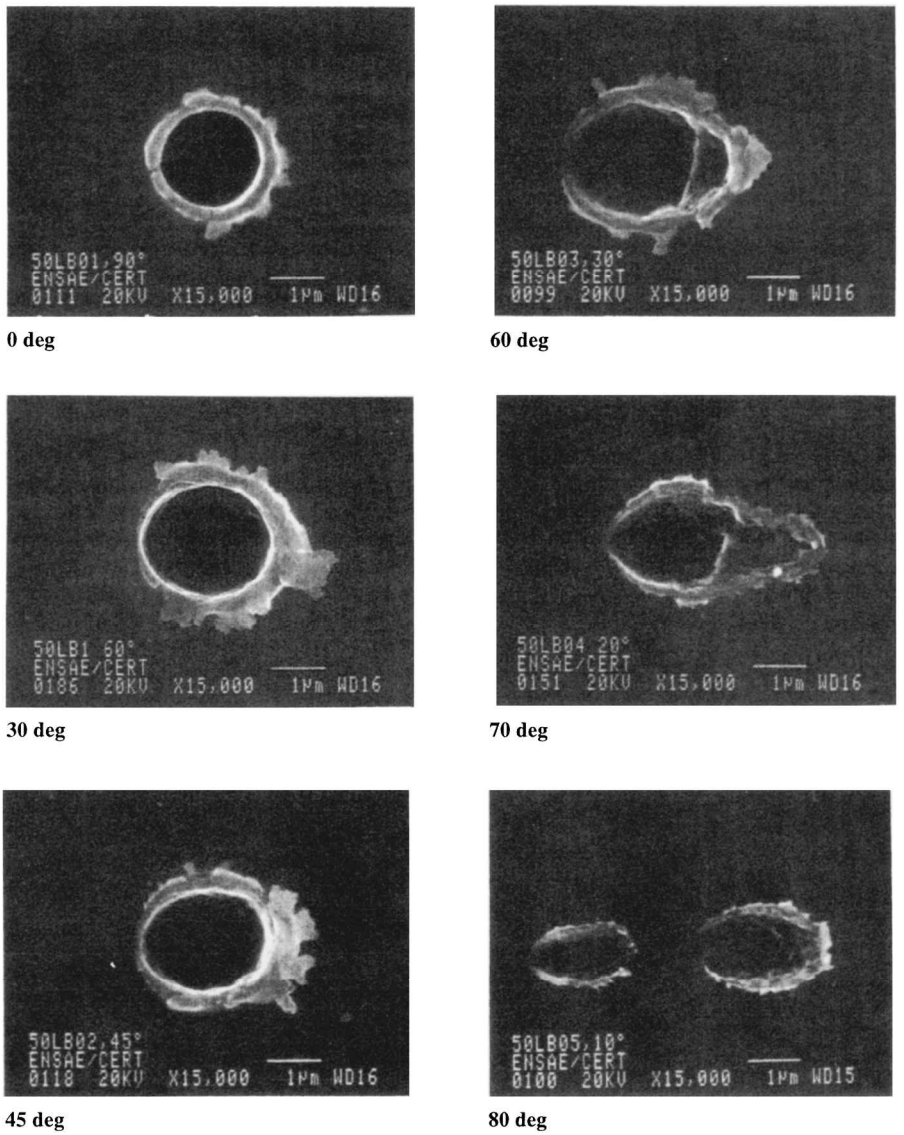

Fig. 11 Oblique craters in Al for increasing impact angle.

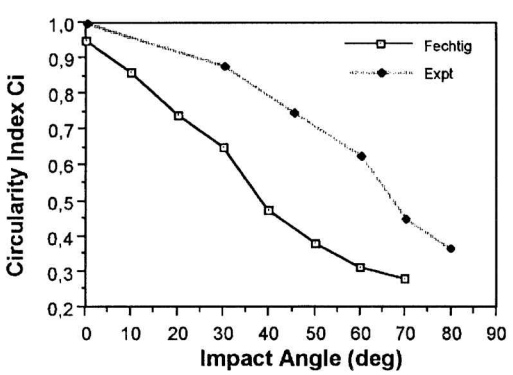

Fig. 12 Variation of Ci with impact angle for glass by Fechtig and our values for Al (Expt).

Table 2 Target material properties

Material	ρ_t, g/cm^3	H, Brinell	c_t, km/s	ε
Al	2.7	90	5.4	0.4

Table 3 Assumed particle properties

	ρ_p (debris), g/cm^3	V (debris), km/s	ρ_p (meteoroid), g/cm^3	V (meteoroid), km/s
Mean for Mir AV side	4.8	7.6	2	19.2
Mean for Mir AR side	4.8	6.4	2	22.6
LDEF row 09	4.8	10.8	2	23.2
LDEF row 03	4.8	0.0	2	17.0

spacecraft. The results can be examined in table form or with the aid of color plots. The flux models used here are Grün's meteoroid model and Kessler's debris model.

The Echantillons experiment module was mounted on the conical part of the Mir orbital station at 45 deg to two solar arrays. Only a simplified version of the core module was modeled, as the rest of the station was too far away to affect the experiment. The LDEF satellite is modeled by a 12-sided cylinder, and the meshing system allows identification of the flux on the different rows. Meteoroid models predict flux as a function of particle mass, and debris models predict flux as a function of particle diameter. To compare observed flux from Mir and LDEF surfaces with the model, we have used the Cour-Palais empirical equation selected in the experimental section. Only the semi-infinite experimental surfaces were used for comparison (this is true everywhere). Table 2 shows the target material properties used in the calculation. The particle properties are given in Table 3, where the velocities were calculated using the ESABASE model.

The model and observed results for the Mir experiment are shown in Fig. 13. The Cour-Palais equation was used to convert d to D. The model prediction underestimates the observed flux by a factor

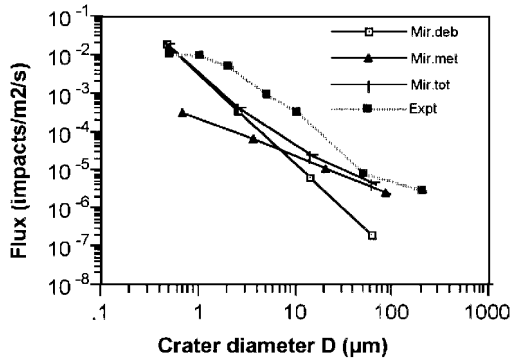

Fig. 13 ESABASE model of Mir meteoroid (Mir.met), debris (Mir.deb), and total (Mir.tot) flux compared with observed values (Expt).

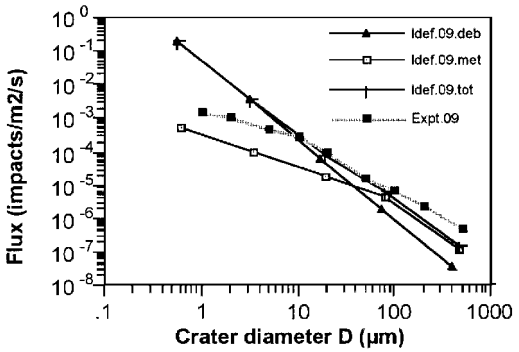

Fig. 14 ESABASE model of LDEF leading-surface meteoroid (ldef.09.met), debris (ldef.09.deb), and total (ldef.09.tot) flux compared with observed values (Expt.09).

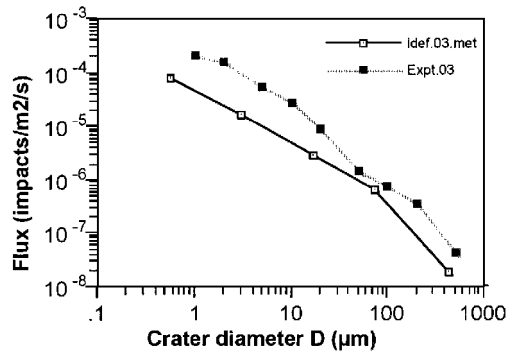

Fig. 15 ESABASE model of LDEF trailing-edge meteoroid flux (ldef.03.met) compared with observed values (Expt.03).

of approximately 6 for crater diameters between 1 and 50 μm. The model does not show the same plateau as the observed data for crater diameters smaller than 1 μm. Similarly, for the leading surface or row 09 of LDEF the model particle diameter and mass values were converted to crater diameters using the Cour-Palais equation. The results are shown in Fig. 14. The graph shows that the experimental data lie between model predictions for meteoroids and debris for crater diameters less than 10 μm. For crater diameters larger than 10 μm, the experimental data approximately follow the total flux, although there is an increasing divergence for larger crater sizes. Apparently, the debris model is predicting too high a flux for small particles. This is consistent with findings by McDonnell[26] and suggests that the micron end of the Kessler debris model needs modification.

Similarly, the crater size distributions found on FRECOPA surfaces can be compared with model data for the trailing edge of LDEF. Figure 15 shows a similar gradient for both model and observed values, but the model predictions are a factor 2–3 lower than the observed values. Even allowing for experimental error, this difference is too large to be ignored. Either the meteoroid model is underestimating the meteoroid flux, or there is a unexpected debris component on the trailing edge. The latter explanation has also been proposed by other investigators.[27,28] These possibilities are debated in the "Discussion."

Discussion

In this section, particular aspects of the results are considered, including impact feature circularity, particle collection methods, and particle fluxes on the LDEF and Mir experiments.

Circularity

This circularity and angle of impact are useful in determining the source of secondary impacts and could possibly be used for determining particle orbits, although this is outside the range of the work presented here. Hydrocode simulations using Autodyn-3D have recently been used to investigate various aspects of oblique impact.[29] Previous work has shown that particle shape influences crater morphology but that it is possible to distinguish between craters formed by oblique impacts and those formed by highly nonspherical particles.[23]

A particularly large number of elliptical craters were found on some Mir samples. Most of these noncircular craters were oriented at approximately 45 deg to the experiment frame with a mean circularity of 0.8. Comparison of this circularity with simulation experiments showed that they came from impacts with an incidence of 40 deg to the target normal. It was found virtually impossible to distinguish whether it was +40 or −40 deg, partly because the craters were so small and partly because the crater lips often gave no clue to direction. We suggest that these were secondary impacts due to a primary impact on a Mir station surface, which sent debris flying towards the experiment module. The primary impact would have to be some distance from the experiment surfaces to explain the uniformity of direction and circularity of the craters. The geometrical model from ESABASE showed that there was a direct line of sight between the Mir experiment and the main body of the station or the middle solar panel. Therefore the primary impact could have occurred on either of these surfaces, both several meters from the experiment module.

Particle Collection Methods

Experience from the LDEF and Mir particle collection methods presented here show the potential of passive semi-infinite and multilayer collection experiments. Passive semi-infinite samples give size and some directional and compositional details. They are robust and reliable and require no power. If materials of high purity are used, material defects are less likely to prejudice crater counts and chemical analysis. If high surface quality (polished) samples are used, smaller impacts can be examined and the size range of flux models might be extended. However, metal targets are not ideal for chemical analysis, as a large proportion of particles vaporize upon impact. For fewer particles to vaporize, a less dense, less resistant medium should be employed. Several research groups are currently developing ultra-low-density media, such as silica aerogels and organic foams, for this purpose.

Passive multilayer detectors also give size and some directional and compositional information. The layers of thin foils serve to decelerate the impactors and to capture the fragments. This method gives superior data for chemical analysis than semi-infinite detectors. However, the interpretation of flux from thin foils can be more involved than that from thick foils, depending on the size of the particle. Much thinner foils than those used on LDEF and Mir would provide excellent particle detectors as they would have a $D/d = 1$ for all but the smallest particles. However, foils thinner than 2 μm are fragile and vulnerable to accidental mishandling.

Mir and LDEF Flux

The Aragatz experiment on Mir showed a much higher flux for some samples on side AV. This was observed only for impact diameters below 10 μm. As previously described, these craters were attributed to secondary impacting, but even when the secondary element had been removed, the average particle flux for Mir was still higher than the model predictions. Initially it was thought that this was due to incorrect modeling of the pointing of the station. But the measured flux was as high as a leading surface; i.e., the maximum possible flux. It is not possible that both faces of the module saw maximum flux. We deduce that the model calculations are underestimating the actual Mir environment. Two possible explanations can be envisaged: either there are more particles at orbits of higher incli-

nations (Divine's interplanetary dust population breakdown shows a distinct inclined component[30]) or the extra particles are due to the dirty environment of a manned station. With the arrival, docking, and departure of several Soyuz and Progress vehicles during the time of exposure, the continual generation of secondary particles would produce more than the predicted amount of space debris impacts.

For LDEF, comparisons for the leading surface show that for crater diameters below 8 μm the modeled flux is higher than the observed flux. Above 8 μm, the model follows the observed flux quite closely. As the observed flux is above that given by the meteoroid model, it seems unlikely that this effect is due to a lower meteoroid flux than calculated. It seem more probable that the debris model is overestimating the amount of debris particles under 8 μm. This was already suspected by Kessler.[31] For the trailing surface the model predicts no debris at all. One could expect the observed distribution shape to follow Grün's meteoroid model, but it clearly does not. The observed data are a factor of 2–5 times higher than the model-predicted meteoroid flux. It appears there is a debris component striking the back of the satellite. Chemical analysis of crater residues on the trailing edge showed evidence of debris particles. This evidence lends weight to the second hypothesis. To strike the trailing edge of LDEF, the debris particles must be in an elliptical orbit around the Earth. One of the most obvious candidates already suggested is particles in geostationary transfer orbit.[28]

Comparison Between LDEF and Mir Results

The two data sets with similar targets invite comparison. The main differences between the LDEF and Mir missions that might have influenced the particle flux were geometry, orientation, altitude, and inclination. Similar targets were used, and it could be argued that the missions occurred almost simultaneously, but the Mir experiments were collecting for a shorter period and on average later than LDEF.

Even when the secondary flux was subtracted, the observed flux on Mir was higher than that on the leading surface of LDEF for $D <$ 50 μm. Considering the orientation difference, it is surprising that the flux on Mir was higher than that on LDEF 09. The flux of smaller particles in the Mir orbit seems to be significantly higher than that in LDEF orbit. Experiments such as the European Space Experiment Facility (ESEF) to be flown on the Mir orbital station from October 1995 as part of the EUROMIR-95 mission could verify these results.

Conclusions

Analysis of impacts on space-exposed samples reveals useful information about the debris and micrometeoroids particle flux in the near-Earth environment. The multilayer detectors revealed that many of the impacting particles were irregularly shaped. The detectors were found to decelerate impacting particles sufficiently for more residues to be found than for normal impacts. High flux values on the trailing edge of LDEF suggest that debris are to be found in elliptical and not just circular orbits. We also learned from the LDEF samples that the Kessler debris model is overestimating the flux for particles smaller than 3 μm in diameter. Kessler based the micron range of the debris model partly on measurements of flux on Solar Max surfaces. These measurements are now considered erroneous because they were probably perturbed by secondary impacts, and the misleading Pailer and Grün equation was used in the conversion of data.

Secondary impacts can easily distort flux measurements, particularly for surfaces near to complex geometries. We found clear evidence of secondary impacting on one side of the Mir experimental module. The orientation and angle of the impacts pointed to a primary impact on the central body of the Mir station or on the central solar panel. Once identified, this secondary flux is easily subtracted from the flux measurements to determine the real flux. Despite this subtraction, the flux observed on the Mir experiment surfaces is higher than that predicted by the models. This difference could be explained either by a general pollution of the environment surrounding the Mir orbital station or by Mir's higher orbital inclination. It is possible that the models do not adequately describe the increase in flux with increasing orbital inclination. It is hoped that future experiments such as ESEF will contribute to these data. We can see that the results obtained confirm the potential of in situ particle detection experiments and add to our knowledge of current and future risks for space missions.

Appendix: Empirical Equations

Numerous empirical and semi-empirical relationships have been developed to convert crater/perforation morphology to particle mass/diameter, equivalent crater size in aluminum, or equivalent penetration thickness. All of these methods depend on certain assumptions about projectile densities, velocities, and interaction with the target. The equations are developed using regression methods to approximate results of laboratory impact experiments. All of the equations given here are semi-infinite equations and are applicable to the semi-infinite or thick target regime where only cratering and no penetration occurs. The equations were developed principally for shielding considerations where the crater depth P was considered the most important parameter. To determine D/d, the ratio P/D must be assumed:

$$P/d = P/D \cdot D/d \tag{A1}$$

Cour-Palais and Christiansen[32] for aluminum targets, 50 μm $< d <$ 1.3 cm and $V <$ 12 km/s:

$$\frac{P}{d} = \frac{5.24 d^{0.056}}{H^{0.25}} \left(\frac{\rho_p}{\rho_t}\right)^{0.5} \left(\frac{V}{c_t}\right)^{0.667} \tag{A2}$$

Pailer and Grün[33] for iron and polystyrene micrometer-sized particles impacting various films and other collected data, $1 \leq V \leq$ 20 km/s:

$$\frac{P}{d} = \left(\frac{0.772}{\varepsilon^{0.06} \rho_t^{0.5}}\right) d^{0.21} \rho_p^{0.73} (V \cos\theta)^{0.88} \tag{A3}$$

NASA[34] for metal targets, where K_∞ is a target material constant (0.42 for aluminum and 0.25 for stainless steel):

$$P/d = K_\infty d^{0.056} \rho_p^{0.519} V^{0.667} \tag{A4}$$

Acknowledgments

The authors thank E. Grün, G. Schaefer, and R. Srama at MPI, Heidelberg, and C. Loupias at Centre d'Etudes de Gramat for their help in conducting tests, the metallurgy laboratory at Sup' Aero for its help in analysis, and J. A. M. McDonnell of the University of Kent and M. Zolensky of NASA Johnson Space Center for contributing samples for analysis.

References

[1] McDonnell, J. A. M., "Microparticle Studies by Space Instrumentation," *Cosmic Dust*, edited by J. A. M. McDonnell, Wiley, New York, 1978.

[2] Hemenway, C. L., Hallgren, D. S., and Kerridge, J. F., "Technical Description of the Gemini S-10 and S-12 Micrometeorite Experiments," *Space Research*, Vol. 8, edited by A. P. Mitra, L. G. Jacchia, and W. S. Newman, North-Holland, Amsterdam, 1968, pp. 521–535.

[3] Nagel, K., Fechtig, H., Schneider, E., and Neukum, G., "Micrometeorite Craters on Skylab Experiment S-149," *Interplanetary Dust and Zodiacal Light: Proceedings of the IAU Colloquium, No. 31* (Heidelberg, Germany), No. 48, Lecture Notes in Physics, edited by H. Elsässer and H. Fechtig, Springer–Verlag, Berlin, 1976, pp. 275–278.

[4] Cour-Palais, B. G., Brown, M. L., and McKay, D. S., "Apollo Window Meteoroid Experiment," *Apollo 16 Preliminary Science Report*, NASA SP-315, Nov. 1972, pp. 26-1–26-10.

[5] Mandeville, J. C., and Lem, H. Y., "Scanning Electron Microscope Analysis and Energy Dispersive X-Ray Analysis of the Surface Features of Surveyor III Television Mirror," *Proceedings of the 3rd Lunar Science Conference*, edited by D. R. Criswell, Vol. 3, MIT Press, Cambridge, MA, 1972, pp. 3201–3212.

[6] Mandeville, J. C., "Microcraters on Lunar Rocks," *Proceedings of the 7th Lunar Science Conference*, edited by R. B. Merrill, Vol. 1, Pergamon, New York, 1976, pp. 1031–1038.

[7] Whipple, F. L., "On Maintaining the Meteoritic Complex," *Zodiacal Light and the Interplanetary Medium*, edited by J. L. Weinberg, NASA SP-150, June 1967, pp. 409–426.

[8] Cour-Palais, B. G., "Meteoroid Environment Model—1969 (Near Earth to Lunar Surface)," NASA SP-8013, March 1969.

[9]Zook, H., Lange, G., Grün, E., and Fechtig, H., "The Interplanetary Micrometeoroid Flux and Lunar Primary and Secondary Microcraters," *Properties and Interactions of Interplanetary Dust*, edited by R. H. Giese and P. Lamy, D. Reidel, Dordrecht, The Netherlands, 1985, pp. 89–96.

[10]Grün, E., Zook, H., Fechtig, H., and Giese, R. H., "Collisional Balance of the Meteoritic Complex," *Icarus*, Vol. 62, No. 2, 1985, pp. 244–272.

[11]Hallgren, D. S., and Hemenway, C. L., "Analysis of Impact Craters from the S-149 Skylab Experiments," *Interplanetary Dust and Zodiacal Light: Proceedings of the IAU Colloquium, No. 31* (Heidelberg, Germany), No. 48, Lecture Notes in Physics, edited by H. Elsässer and H. Fechtig, Springer–Verlag, Berlin, 1976, pp. 270–274.

[12]Warren, J., Zook, H., Alton, J. H., Clanton, U. S., Dardano, C. B., Holder, J. A., Marlow, R. R., Schultz, R. A., Watts, L. A., and Wenworth, S. J., "The Detection and Observation of Meteoroid and Space Debris Impact Features on the Solar Max Satellite," *Proceedings of the 19th Lunar and Planetary Science Conference*, edited by G. Ryder and V. L. Sharpton, Vol. 1, Cambridge Univ. Press, New York, 1989, pp. 641–657.

[13]McKay, D. S., "Microparticle Impacts in Space: Results from Solar Max Satellite and Shuttle Witness Plate Inspections," NASA/SDIO Space Environment Effects and Materials Workshop, NASA CP-3035, Pt. 1, 1989, pp. 301–316.

[14]Kessler, D. J., "Orbital Debris Issues," *Advances in Space Research*, Vol. 5, No. 2, 1985, pp. 3–10.

[15]Anderson, B. J. (ed.), and Smith, R. E. (compiler), "Natural Orbital Environment Guidelines for Use in Aerospace Vehicle Development," NASA TM-4527, June 1994.

[16]McDonnell, J. A. M., "Factors Affecting the Choice of Foils for Penetration Experiments in Space," *Space Research*, Vol. 10, edited by R. L. Smith-Rose, North-Holland, Amsterdam, 1970, pp. 314–325.

[17]Mandeville, J. C., "Aragatz Mission Dust Collection Experiment," *Advances in Space Research*, Vol. 10, No. 3–4, 1990, pp. 397–401.

[18]Zolensky, M., Atkinson, D., See, T., Allbrooks, M., Simon, C., Finckenor, M., and Warren, J., "Meteoroid and Orbital Debris Record of the Long Duration Exposure Facility's Frame," *Journal of Spacecraft and Rockets*, Vol. 28, No. 2, 1991, pp. 204–209.

[19]McDonnell, J. A. M., Deshpande, S. P., Niblett, D. H., Neish, M. J., and Newman, P. J., "The Near Earth Space Environment—An LDEF Overview," *Advances in Space Research*, Vol. 13, No. 8, 1993, pp. 87–101.

[20]Lane, G. S., "The Application of Stereographic Techniques to the Scanning Electron Microscope," *Journal of Physics E*, Vol. 2, 1969, pp. 565–569.

[21]Horz, F., Cintala, M., Bernhard, R. P., and See, T. H., "Dimensionally Scaled Penetration Experiments: Aluminum Targets and Glass Projectiles 50 μm to 3.2 mm in Diameter," *International Journal of Impact Engineering*, Vol. 15, No. 3, 1994, pp. 257–280.

[22]Barrett, R. A., Dodson, A. L., Thomas, K. L., Warren, J. L., Watts, L. A., and Zolensky, M. E., "Cosmic Dust Catalog—Volume 13," Solar System Exploration Div., NASA Johnson Space Center, JSC Rept. 25980, Houston, TX, Sept. 1992.

[23]Berthoud, L., "Micrometeoroids and Orbital Debris Observed in LEO," Ph.D. Thesis, L'Ecole Nat. Sup. de l'Aeronautique et de l'Espace, Toulouse, France, Dec. 1993.

[24]Fechtig, H., Nagel, K., Stähle, V., Grogler, N., Schneider, E., and Neukum, G., "Impact Phenomena on an Apollo 12 Sample," *Proceedings of the 8th Lunar Science Conference*, edited by R. B. Merrill, Vol. 1, Pergamon, New York, 1977, pp. 889–899.

[25]Drolshagen, G., "Meteoroid/Debris Impact Analysis Application to LDEF, Eureca and Columbus," *Proceedings of the 1st European Conference on Space Debris*, ESA SD-1, ESOC, Darmstadt, Germany, 1992, pp. 515–522.

[26]McDonnell, J. A. M., "Impact Cratering from LDEF's 5.75-yr Exposure: Decoding of the Interplanetary and Earth-Orbital Populations," *Proceedings of the Lunar and Planetary Science*, edited by G. Ryder and V. L. Sharpton, Vol. 22, Lunar and Planetary Inst., Houston, TX, 1991, pp. 185–193.

[27]Horz, F., Bernhard, R. P., See, T. H., and Brownlee, D. E., "Natural and Orbital Debris Particles on LDEF's Trailing and Forward-Facing Surfaces," *Proceedings of the 3rd LDEF Post-Retrieval Symposium*, edited by A. S. Levine, NASA CP-3275, Pt. 1, Feb. 1995, pp. 415–429.

[28]Kessler, D. J., "Origin of Orbital Debris Impacts on LDEF's Trailing Surfaces," *Proceedings of the 2nd LDEF Post-Retrieval Symposium*, edited by A. S. Levine, NASA CP-3194, Pt. 2, April 1993, pp. 585–593.

[29]McDonnell, J. A. M., Gardner, D. G., Newman, P. J., Robertson, N. J., and Hayhurst, C. J., "Hydrocode Modelling in the Study of Space Debris Impact Crater Morphology," *Proceedings of the 1st European Conference on Space Debris*, ESA SD-1, ESOC, Darmstadt, Germany, 1992, pp. 425–431.

[30]Divine, N., Grün, E., and Staubach, P., "Modeling the Meteoroid Distribution in Interplanetary Space and Near-Earth," *Proceedings of the 1st European Conference on Space Debris*, ESA SD-1, ESOC, Darmstadt, Germany, 1992, pp. 245–250.

[31]Kessler, D. J., "Orbital Debris Environment for Spacecraft in LEO," *Journal of Spacecraft and Rockets*, Vol. 28, No. 3, 1991, pp. 347–351.

[32]Cour-Palais, B. G., "Hypervelocity Impacts in Metals, Glass and Composites," *International Journal of Impact Engineering*, Vol. 5, 1987, pp. 681–692.

[33]Pailer, N., and Grün, E., "The Penetration Limit of Thin Films," *Planetary Space Science*, Vol. 28, No. 3, 1980, pp. 321–331.

[34]Frost, V. C., "Meteoroid Damage Assessment," NASA SP-8042, May 1970.

F. S. Milos
Associate Editor